Submitted: 11. 11. 2023.

Accepted: 29. 11. 2023.

https://doi.org/10.2298/SOS231111064D

The effect of particle size on the crystallization $LiGe_2(PO_4)_3$ phase from glass

Nataša G. Đorđević[1,*], Srđan D. Matijašević[1], Slavica R. Mihajlović[1], Jovica N. Stojanović[1], Aleksandra M. Radulović[2], Ljiljana B. Savić[3]

[1]*Institute for Technology of Nuclear and Other Mineral Raw Materials (ITNMS), 86 Franchet d Esperey St., 11000 Belgrade, Serbia*

[2] *Institute of General and Physical Chemistry, 12 Studentski Trg,11000 Belgrade, Serbia*

[3]*Faculty of Technical Sciences, Kosovska Mitrovica, University of Pristina situated in Kosovska Mitrovica, 7 Knjaza Milosa St., 38220 Kosovska Mitrovica, Serbia*

*Corresponding author: n.djordjevic@itnms.ac.rs

Abstract:

The glass was prepared by the standard melt-quenching technique. The crystallization of powder glass from the system Li_2O-Al_2O_3-GeO_2-P_2O_5 was studied. The investigations were performed under non-isothermal and isothermal conditions using the AAS, DTA, XRD and FTIR methods. The aim of this research was to study the ease of glass formation, crystallization and crystal structure of obtained phases. The results showed that the glass crystallizes by primary crystallization. $LiGe_2(PO_4)_3$ was formed as the primary phase, until detectable traces of GeO_2 were formed as secondary. The influence of particle size of the glass powder samples in the range 0-1 mm on the temperature of the DTA crystallization peak, T_p, the peak height $(\delta T)_p$ and the parameter $T_p^2/(\Delta T)_p$ was studied. It was demonstrated that for the particle size in the range of 0.05-0.35 mm surface and volume crystallization were significant, while the particle size >0.35 mm according to the volume crystallization was dominant.

Keywords: *particle size, glass crystallization, structure*

1. Introduction

The studies of crystallization of Li_2O-Al_2O_3-GeO_2-P_2O_5 glasses showed that the $LiGe_2(PO_4)_3$ phase which belongs to the solid electrolyte was formed [1]. The crystal structure of $LiGe_2(PO_4)_3$ consists of a three-dimensional framework of corner-shared GeO_6 octahedra and PO_4 tetrahedra [2]. Each GeO_6 octahedron is connected to three PO_4 tetrahedra, and each of them is linked to four GeO_6 octahedra. These units, in turn, are connected in such manner to form "ribbons" along the c-axis and the ribbons are joined together along the a- and b-axis by PO_4 tetrahedra [3].

This family of crystalline phosphates is often referred to as "NASICONs" (an acronym for "Na-Super Ionic Conductors") although they do not contain Na+ ions [4]. NASICON-type materials are found as a solid electrolytes candidates for utilization in high-energy-density batteries, supercapacitors, sensors, displays, nuclear waste disposals, low-expansion ceramics, thermal-shock-resistant materials, and electrochemical devices [5].

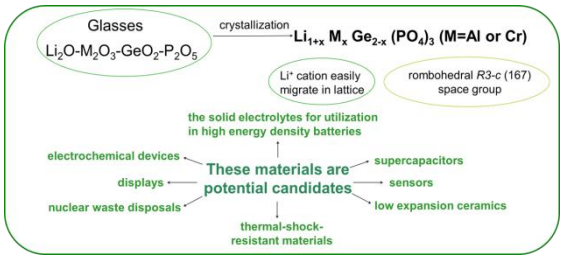

Fig. 1. Potential application of NASICON-type materials

Depending on the composition, the crystal structure can be rhombohedral with R-3C space group, monoclinic with space group C2/c, triclinic, orthorhombic, and corundum-like [4]. Numerous studies were focused on the synthesis path for lithium-ion conductors obtainemnet. Li^+ ion conductors is a huge investigation area with a variety of different compaunds present which constantly attracts investigators. One represntative of Li^+ ion conductors is NASICON type $LiGe_2(PO_4)_3$ [6]. Nasicons can be synthesized by the conventional ceramic method, glass-ceramics method, solution-sol-gel method, or hydrothermal method. In comparison with sintered materials, glass-ceramics have many

advantages because they can be easily manufactured into desired size or shape and have dense microstructure.

In the present paper, the mechanism and influence of the particle size on the crystallization of germanophosphate glass under nonisothermal conditions were studied.

2. Experimental procedure

The glass was prepared by melting a homogeneous mixture of reagent-grade Li_2CO_3, Al_2O_3, GeO_2, and $(NH_4)_2HPO_4$ in a covered platinum crucible. The components were thoroughly mixed and heated stepwise up to 300°C to remove volatile substances. The melting was performed in an electric furnace BLF 17/3 at T=1400 °C during t=0.5 h. The melt was cast and cooled between two steel plates.

The chemical analysis was performed using an atomic absorption method with the spectrophotometer AAS PERKIN ELMER Analyst 300. The measurement uncertainty was 0.49%.

The experiments under non-isothermal heating conditions were performed using a differential thermal analysis method on a device Netzsch STA 409 EP where Al_2O_3 powder was the reference material. Powder samples of the following granulations were prepared: <0.048; 0.048-0.063; 0.063-0,1; 0.1-0.2; 0.2-0.3; 0.3-0.4; 0.4-0.5; 0.5-0.65; 0.65-0.83 and 0.83-1.0 mm. The glass powders were prepared by crushing bulk glass in an agate mortar and sieving it to the fractions with appropriate grain size. In the experiments, a constant weight (100 mg) of the samples were heated at a heating rate β =10°C/min to T=1100°C. The experiments with bulk glass samples were performed in an one-stage regime. The samples were heated in an electric furnace Carbolite CWF 13/13, with automatic regulation and temperature accuracy of ± 1°C, at a heating rate β = 10°C/min up to the chosen crystallization temperature at which they were maintained over 100 h. Finally, the samples were removed from the furnace, cooled and then crushed in the agate mortar. The schematic experimental flow chart is shown in Fig. 2.

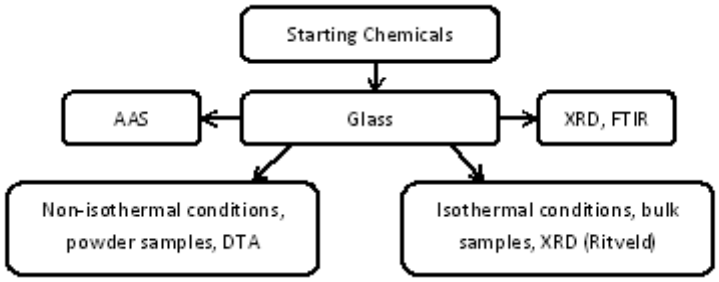

Fig. 2. Experimental flow chart

Powdered samples were used for X-ray diffraction (XRD) analysis. The XRD method was used to determine the phase composition and the XRD patterns were obtained using a Philips PW-1710 automated diffractometer. All the XRD measurements were performed at room temperature in a stationary sample holder. The LSUCRIPC program was used for the refinement of the cell dimensions from the powder data [7]. The quantitative amounts of the crystalline phases in the sample were determined using the full structure matching mode of the Rietveld refinement method [8], using the the FULLPROF program [9]. The standard database (JCPDS database) for XRD patterns was used for phase identification. Detection limit was below 2%.

Infrared (IR) transmission spectra of the glasses and crystals were recorded from 4000 to 400 cm^{-1} using Perkin–Elmer 2000 FTIR spectrometer. IR spectra of the glass were recorded in KBr pellets.

3. Results and discussion

Choosing the particular glass, the starting point was the composition $Li_{1+x}Al_xGe_{2-x}(PO_4)_3$, where x is stoichiometric values. Recent studies showed that during the crystallization of a glass with similar composition, $LiGe_2(PO_4)_3$ was formed as a phase with NASICON structure [6]. Preliminary experiments were performed and based on the results of these experiments, the composition with x=0.8 was chosen.

The results of the chemical analysis show that a glass composition of $6.4Li_2O{\cdot}8.6Al_2O_3{\cdot}42GeO_2{\cdot}43P_2O_5$ (wt%) was obtained. Powder X-ray diffraction (XRD) analysis confirmed that an amorphous structures were obtained. No peaks attributed to any crystallized compound could be identified except a broad diffraction halo, which is attributed to the glassy amorphous phase (figure not shown). The samples were

transparent, without visible residual gas bubbles. In Fig. 3, the differential thermal analysis (DTA) curve of glass sample particle sizes of < 0.048 mm, 0.3-0.4 mm and 0.83-1 mm, recorded at a heating rate of β=10 °C/min in the temperature range T=400-800°C is shown.

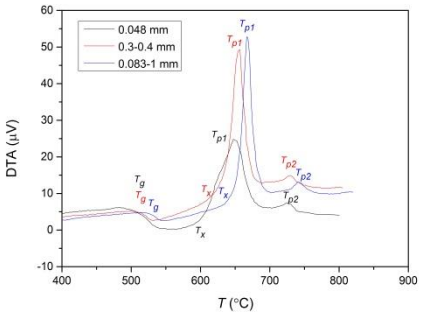

Fig. 3. DTA curves recorded at a heating rate of β=10°C/min for powder sample particle sizes: a) <0.048 mm, b) 0.3-0.4 mm and c) 0.83-1 mm.

On Fig. 3, it can be noticed four thermal events. They ascribe on the picture: the glass transition temperature (T_g), onset crystallization temperature (T_x) and endothermic peaks (T_{p1}, T_{p2}). As can be seen in Fig. 3, six exothermal temperature peaks for all curves were registered. The intensive peaks appeared at lower temperatures (T_{p1}-648, 657 and 667°C). Also, only the peaks intensity is changed with particulate size while their positions do not change markedly by increasing the glass particle size. Similar peaks behavior were registered for all glass samples studied.

To identify the formed crystalline phases at the temperatures corresponding to peak T_{p1} and T_{p2} (725, 729 and 743°C), the experiments under isothermal conditions were performed with bulk samples. In a one-step regime, the samples were heated to form two phases separately at crystallization temperatures from DTA analysis. The XRD patterns of these samples showed that first was formed a $LiGe_2(PO_4)_3$ -JCPDS 80-1922, rhombohedral, space group $R\bar{3}c$ (167) as primary (T_{p1}), and then GeO_2-JCPDS 83-0543, hexagonal, space group $P3_221$ (152) as secondary ones (T_{p2}) [10,11]. To determine quantitatively the ratio of the crystalline phases, a sample was heated at T = 800°C for t = 100 h. A Rietveld profile matching mode fitting plot of this sample is presented in Fig. 4, while the results of the fitting are shown in **Tab. I**.

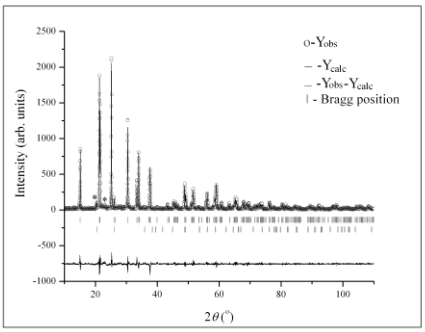

Fig. 4. Rietveld refinement plot of glass sample heat-treated at T = 800°C for t = 100 h. Observed (o), calculated (—), and difference powder diffraction profiles. Vertical bars mark Bragg's peak positions.

Tab. I The most important crystallographic parameters for crystalline phases, obtained from Rietveld refinement of XRD pattern [3].

Phase	Unit cell parameters			Reliability factors		Vol. frac. (%)
	a (Å)	*b* (Å)	*c* (Å)	R_B(%)	R_F(%)	
$LiGe_2(PO_4)_3$	8.2648(2)	8.2648(2)	20.5696(7)	7.83	6.58	97.6
GeO_2	5.003(2)	5.003(2)	5.580(5)	8.83	18.80	2.4

The obtained results show that this glass crystallized into a two-component glass–ceramic, with $LiGe_2(PO_4)_3$ (97.6 vol%) as the primary phase, and GeO_2 (2.4 vol%) as the secondary ones. The phase GeO_2 is formed as a β-modification (hexagonal, space group $P3_221$ (152) whose melting temperature is $T_{GeO2\text{-}\beta}$=1116°C [10].

With the addition of Al_2O_3, Ge^{+4} cations are replaced by Al^{+3} in the network and there is a lack of positive charge that is compensated by Li+ ions, leading to the following structure $Li_{1+x}Al_xGe_{2-x}(PO_4)_3$. Also, the thermal stability of the structural glass network increases. In the case of the tested composition, Al is found in the structure below the detection limit of XRD analysis. The calculated unit-cell parameters were in good agreement with the literature data and no divergence was registered [12]. This suggests that the Al^{3+} ion present in the glass (4.4%) was not incorporated into the structure of the formed phases by replacing the Ge^{4+} ion, because in that case, the crystallographic parameters would differ from the literature data [13]. In this composition, P is a glass former and alkali oxides are glass modifiers. Undersuitable conditions and depending on the nature of oxide like Al_2O_3, this composition can give rise to glassy materials [4].

Based on these considerations, it can be concluded that the obtained glass-ceramic has a high content of $LiGe_2(PO_4)_3$ phase and a minor presence of GeO_2 phase, so the processes of nucleation and crystal growth in this glass can be attributed mainly to the formation of the $LiGe_2(PO_4)_3$ phase.

The glasses generally crystallize by either surface or volume mechanism. One of the procedures convenient for evaluating the dominant crystallization mechanism of glass powder besides optical microscopy is differential thermal analysis (DTA) [14]. Experimental and theoretical studies have shown that the particle size of glass powder influences the mechanism of its crystallization [15,16]. In Fig. 5, the effects of particle size on the exothermal DTA peak temperatures, T_p, for all samples are presented. It can be seen (Fig.5) that the resistance to crystallization of the tested glass increases with the increase of the glass powder size, passing through the maximum value for the sample of the largest granulation. This indicates a dominant crystallization model in this glass.

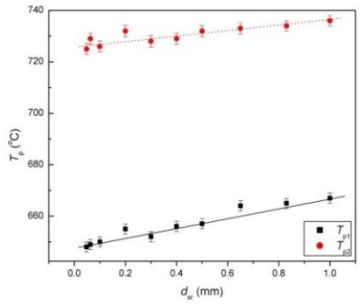

Fig. 5. The Effect of particle size on DTA exothermal peak temperatures T_p

The parameters of $T_p^2/(\Delta T)_p$ and $(\delta T)_p$ show the dependency on particle size and can be used as a qualitative measure for the polymorphic as well as the primary surface and volume crystallization [17]. The ratio $T_p^2/(\Delta T)_p$, where T_p is the DTA peak temperature and $(\Delta T)_p$ is the half-width of the DTA peak is related to the dimension of crystal growth. The height of the exothermal DTA peak $(\delta T)_p$ is proportional to the total number of nuclei (volume and surface) contained in the glass particle. If surface and volume crystallization proceed simultaneously, three distinct regions can be distinguished as a function of particle size. They reflect the behavior arising from decreasing surface-to-volume ratio with the increase in particle size.

The results of the influence of particle size on the ratio $T_p^2/(\Delta T)_p$ and DTA peak height $T_p^2/(\Delta T)_p$ for peak 1 are shown in Fig. 6.

As can be observed from Fig. 6. (peak 1), the curves with two distinguishable regions were obtained (<0.35 mm, ≥0.035 mm). The ratio $T_p^2/(\Delta T)_p$ and $(\delta T)_p$ have the lowest values for average particle size <0.050 mm.

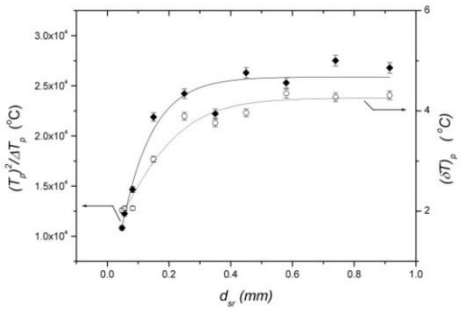

Fig. 6. The effect of particle size on $T_p^2/(\Delta T)_p$ and $(\delta T)_p$ for peak 1.

Practically, only for this glass grain size the number of surface nuclei was comparable with volume ones and the total number of the present nuclei is the smallest. In the particle size range of 0.05-0.35 mm, both parameters increased to asymptotic values. In this case, with increasing particle size, the ratio of volume to surface nuclei increased as the number of volume nuclei increases with respect to the number of surface nuclei. Both mechanisms of crystallization are present also in this range. In the grain size range ≥0.35 mm, both parameters remain approximately constant (Fig.6). In this case, the number of volume nuclei dominates in the total number of nuclei and hence, the volume crystallization mechanism prevails. When the number of volume nuclei becomes dominant, a further increase in particle size does not significantly influence the change in the volume nuclei or the total number of nuclei.

The resistance of a obtained glass to the crystallization process can be determined based on the change in the maximum or shape of the crystallization peak. Several parameters derived from the DTA curve can be used to describe the resistance of glass to crystallization during heating based on characteristic temperatures (T_g – glass transition temperature, T_x – onset crystallization temperature, T_p – crystallization temperature, and T_m – melting temperature).

The temperature difference by Angell, $K_2 = T_x - T_g$ [18,19] (1)

is a good indication of thermal stability because the higher the value of this difference, the more delay is present in the nucleation process. Hruby criterion, among several parameters for glass stability (GS) assessment, is most frequently used [20,21]:

$$K_H = \frac{T_x - T_g}{T_m - T_X} \quad (2)$$

In **Tab. 2**, these temperatures and other characteristic DTA temperatures, glass transformation temperatures T_g, onset crystallization temperature (T_x), crystallization temperature T_p and glass melting temperatures T_m were summarized. Also, the reduced glass transition temperatures [22], $T_{rg} = \frac{T_g}{T_m}$ (3)

and Hruby, as well as Angel K_2 parameters are shown in Table 2.

Tab. II DTA temperatures and the parameters calculated for glass powder sample particle sizes 0.048, 0.3-0.4 and 0.083-1mm, heated at β=10°C/min.

p.size (mm)	T_g	T_x	T_{p1}	T_{p2}	T_m	T_{rg}	K_H	K_2
0.048	511	605	648	725	1061	0.48	0.21	94
0.3-0.4	512	608	657	729	1068	0.48	0.21	96
0.083-1	527	636	667	743	1082	0.49	0.24	112

Glass forming ability (GFA), as related to the ease of vitrification, is vital for understanding the origin of glass formation and is important for designing glasses. The glass transition temperature represents the strength or rigidity of the glassy structure. The value of reduced glass transition temperature T_{rg} indicates a small glass-forming tendency of this glass. According to different studies, the higher the values of Angell (K_2) and Hruby (K_H), parameters for a certain glass, the higher its stability against crystallization on heating.

Due to the (K_2) and K_H, parameters, this glass revealed high crystallization ability during heating, also the largest particle size of glass (0.83-1 mm) is more stable than lower (0.048 mm) against crystallization. It can be seen also from the analysis of the Fig.3, the larger the size of the glass particles, the larger the peak area, i.e. the required energy for the crystallization process. As well, according to the values of the Angell parameter (K_2, Tab. II), the process of nucleation can be independent of crystallization and this glass can be suitable for engineering and manufacturing [21,23].

Infrared spectroscopic studies make it possible to better understand the structure at a short distance of the investigated glass. When analyzing the infrared spectrum of the test glass, Fig. 7, can be observed three characteristic areas:3700-1800 cm^{-1},1800-1400 cm^{-1}, and 1400-400 cm^{-1}.

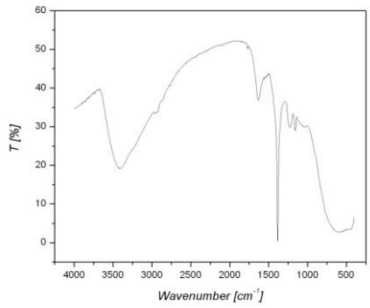

Fig. 7. IR spectra of test glass powder.

A band at 1630 cm^{-1}, represents an area H-O-H bending of water molecules [24]. The frequencies that appear in the first field are characteristic of systems that contain bound water. The sharp absorption band at ~ 1380 cm^{-1} can be found in the glass hygroscopic and it is derived from strain P-OH of the adsorbed water on the glass sample [25]. In area 1800-1400 cm^{-1}, there is the free vibration of the water molecule. The vibratory modes which occur in the area of 1250-900 cm^{-1} are intramolecularly elongated [PO_4] tetrahedral vibrations [5].

Also in the area of 650-400 cm^{-1}, which occurs in the wide band comes from the angle deformation of the tetrahedron O-P-O. In the area between 800-500 cm^{-1}, vibration bands occur originating from the asymmetric and symmetric stretching Ge-O-Ge bridges connecting [GeO_6] octahedra [26]. It can be concluded that a wide band, which occurs in the area of 1000-400 cm^{-1} is the area of the vibration [PO_4] and [GeO_6] of structural units of the glass. It may be considered that the crystal structure of the main crystal phase $LiGe_2(PO_4)_3$ of this glass sample consists of GeO_6 octahedra and PO_4 tetrahedra.

The crystal structure of the $LiGe_2(PO_4)_3$ phase is shown in Fig. 8, in a representation that indicates the polyhedral arrangement of oxygen atoms around the cations. The structure can be described as a covalent skeleton $[Ge_2P_3O_{12}]^-$ constituted of [GeO_6] octahedra and of [PO_4] tetrahedra (Fig. 8). Both units are linked by their corners to form 3D interconnected channels and interstitial spaces where Li^+ cations are distributed.

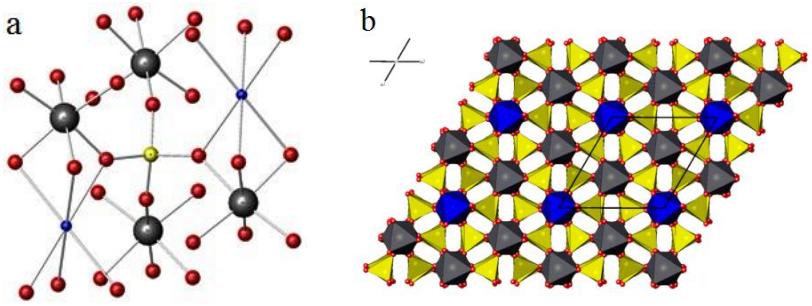

Fig. 8. Schematic representation of the structural unit of the $LiGe_2[PO_4]_3$ phase, left a) phosphorous atoms are schematically represented by yellow, germanium by gray, oxygen by red, and lithium by blue spheres, right b) schematic view along the b-axis showing the polyhedral representation: gray $[GeO_6]$ distorted octahedra, yellow $[PO_4]$ tetrahedral, (blue) $[LiO_6]$ distorted trigonal prism (conducting channels with cavities containing lithium ions, ATOMS V.6.3.1 by FullProf Suite).

Lithium cations compensate for the negative charge of the covalent skeleton $[Ge_2P_3O_{12}]^-$ [13]. Conducting cations can diffuse from one conducting site to another through bottlenecks whose nature depends on the nature of the ions that make up the skeleton and the concentration of conducting ions in the interstitial sites. The change in lattice size directly influence on the size of the pathway for the conducting cations and the hopping distance of the Li^+-ions to the next interstitial space [27]. The ionic transport occurs primarily from the motion of interstitial species depending on cation concentration. Li^+-ions diffuse mainly by an interstitial mechanism due to their small radius (90 pm). Conductivity measurements show the glass-ceramics containing $LiGe_2(PO_4)_3$ phase are excellent lithium ion conductors [28,29].

4. Conclusion

The crystallization of the $6.4Li_2O{\cdot}8.6Al_2O_3{\cdot}42GeO_2{\cdot}43P_2O_5$ (wt%) glass powders was studied. The results showed the primary crystallization of this glass. $LiGe_2(PO_4)_3$ was formed as the stable primary phase, and as a secondary one, the GeO_2 in traces appeared. The effect of the particle size of glass on the crystallization mechanism was analyzed. For particle size in the range of 0.05-0.35 mm both surface and volume crystallization are significant, while for particle size >0.35 mm volume crystallization is dominant. Small

glass-forming tendencies for LAGP glass have been found using the DTA method. IR spectra confirm that structural units of glass skeleton $[Ge_2P_3O_{12}]^-$ consist of Ge-octahedra and P-tetrahedra.

Acknowledgment

The authors are grateful to the Ministry of Education, Science and Technological Development of the Republic of Serbia for the financial support (grant contract No.: 451-03-47/2023-01/200023).

5. References

1. F.Zheng, M.Kotobuki, S.Song, M.O.Lai, L.Lu, J. Power Sources, 389 (2018) 198-213.
2. P.P.Kumar, S.Yashonati, J.Chem.Sci., 118 (2006) 135-154.
3. J. D. Nikolić, S. V. Smiljanjić, S. D. Matijašević, V. D. Živanović, M. B. Tošič, S. R. Grujić, J. N. Stojanović, Process. Appl. Ceram., 7(4) (2013) 147-151.
4. N.Anantharamulu, K.K.Rao, G.Rambabu, B.V.Kumar, V.Radha, M.Vithal, J.Mater.Sci. 46 (2011) 2821-2837.
5. K.Arbi, M.Ayadi-Trabelsi, J.Sanz , J.Mater.Chem., 12 (2002) 2985-2990.
6. J. Fu, Solid State Ionics, 104 (1997) 191-194.
7. R. Garvey, LSUCRIPC Least Square Unit Cell Refinement with Indexing on the Personal Computer, Pow. Diffraction 1 (1986) 114.
8. H.M. Rietveld, J.Appl. Cryst. 2 (1969) 65.
9. J. Rodriguez-Carvajal, "User's guide to program FULLPROF", 2004-LLB-JRC (Laboratorie León Brillouin, CEA-CNRS, Centre d'Etudes de Saclay, Gif sur Yvette, France), 1995.
10. Powder Diffraction File, Card No. 80-1922. Joint Committee on Powder Diffraction Standards (JCPDS), Swarthmore, PA.
11. Powder Diffraction File, Card No. 83-0543. Joint Committee on Powder Diffraction Standards (JCPDS), Swarthmore, PA.
12. H.Yamamoto, M.Tabuchi, T.Takeuchi, H.Kageyama, O.Nakamura, J.Power Sources 68 (1997) 397-401.

13. P. Maldonado-Manso, E.R.Losilla, M. Martinez-Lara, M.A.G.Aranda, S.Bruque, F.E. Mouahid, M.Zahir, Chem. Mater., 15 (2003) 1879-1885.
14. A. R. Boccaccini, B. Hamann, J. Mater. Sci. 34 (1999) 5419-5436.
15. C.S.Ray,Q.Yang, W.Haung, D.E.Day, J.Am.Ceram.Soc. 79 (1996) 3155-3160.
16. S. D. Matijašević, S. R. Grujić, V. S. Topalović, J. D. Nikolić, S. V. Smiljanić, N. J. Labus, V. V. Savić, Sci. Sinter., 54(3) (2022) 321-334.
17. M. B. Tošić, V. D. Živanović, S. R. Grujić, J. N. Stojanović, J. D. Nikolić, J. Non-Cryst. Solids, 354 (2008) 3694-3704.
18. V. Topalović, J. Nikolić, S. Matijašević, J. Stojanović, A. Karamanov, S. Grujić, S. Jevtić, J. Therm. Anal. Calorim., 148(3) (2023) 721-732.
19. M. Nascimento, L. Souza, E. Ferreira, E. Zanotto, J. Non-Cryst Solids, 351 (2005) 3296–3308.
20. A. Kozmidis-Petrovic, J. Šesták, J. Therm. Anal. Calorim., 110 (2012) 997–1004.
21. S. D. Matijašević, S. R. Grujić, V. S. Topalović, J. D. Nikolić, S. V. Smiljanić, N. J. Labus, V. V. Savić, Sci. Sinter., 50(2) (2018) 193-203.
22. S. D. Matijašević, V. S. Topalović, S. R. Grujić, V. V. Savić, J. D. Nikolić, N. J. Labus, S. N. Zildžović, Sci. Sinter., 53(3) (2021) 301-310.
23. S. D. Matijašević, V. S. Topalović, V. V. Savić, N. J. Labus, J. D. Nikolić, S. N. Zildžović, S. R. Grujić, Sci. Sinter., 55(4) (2023) DOI:10.2298/SOS22080922M https://doi.org/10.2298/SOS220809022M
24. K. J. Rao, K. C. Sobha, S. Kumar, Proc. Indian Acad. Sci. (Chem. Sci.), 113(5-6) (2001) 497-514.
25. G. Monteiro, L. F. Santos, J. C. G. Pereira, R. M. Almeida, J. Non-Cryst. Solids, 357 (2011) 2695-2701.
26. M. Alami, R. Brochu, J. L. Soubeyroux, P. Gravereau, G. L. Flem, P. Hagenmuller, J. Solid State Chem., 90 (1991) 185-193.
27. M. Guin, F. Tietz, O. Guillon, Solid State Ionics, 293 (2016) 18-26.
28. M.Cretin, P.Fabry, J.Eur.Ceram.Soc., 19 (1999) 2931-2940.
29. Y. Cui, M. M. Mahmoud, M. Rohde, C. Ziebert, H. J. Seifert, Solid State Ionics, 289 (2016) 125-132.

***Сажетак*:**

Стакло је припремљено стандардном техником, наглим хлађењем растопа стакларске смеше. Проучавана је кристализација стакленог праха из система Li_2O-Al_2O_3-GeO_2-P_2O_5. Истраживања су обављена у неизотермским и изотермским условима. Коришћене су методе AAS, DTA, XRD и FTIR. Циљ овог истраживања био је проучавање могућности формирања стакла, кристализације и структуре насталих фаза. Резултати су показали да стакло кристалише примарном кристализацијом. Као примарна фаза при топлотној обради формирана је $LiGe_2(PO_4)_3$ фаза, док су детектовани и трагови GeO_2 као секундарне фазе. Испитиван је утицај величине честица узорака стакленог праха у опсегу 0-1 мм на температуру ДТА кристализационог пика, T_p, висину пика, $(\delta T)_p$ и параметар $T_p^2/(\Delta T)_p$. Показано је да у распону величине честица 0.05-0.35 мм присутна површинска и запреминска кристализација стакла, док је при величини честица >0.35 тт запреминска кристализација доминантна.

***Кључне речи**: величина честица, кристализација стакла, структура;*